A Novel Inductive Sensor Input Circuit with Improved Tolerance to Non-Concentricity with Touch-Down Bearings

Richard Jayawant [1], Andrea Masala [1], Roy Leung [1], Nigel Davies [1]
[1] Waukesha Magnetic Bearings, Unit J, Downlands Bus. Pk. Lyons Way, Worthing, W. Sussex, UK.
rjayawant@doverprecision.com

Abstract

When using inductive sensors, non-concentricity between the sensor and touch-down bearing stators of an active magnetic bearing (AMB) system can result in the sensor signal being "offset" within the touch-down bearing clearance. The resulting signal will have a larger amplitude at the extremes of motion compared to a well-centered system. A novel signal conditioning circuit is presented which allows the signal to be "re-centered" prior to demodulation. The impact of this circuit on required machining tolerances and sensor noise levels is discussed. We also present an implementation that is well-suited to automated and remote commissioning and the techniques used to set up the sensor sub-system during such a commissioning.

1 Conventional Inductive Sensor Signal Conditioning

Inductive sensors have common usage in AMB systems due to their non-contacting measurement capability, simple and robust construction, acceptable bandwidth and their low conductor count. Inductive sensors have been described by Traxler and Maslen, (Traxler, 2009) but we will recap some of the key elements.

Inductive sensors are typically built into a sensor ring, which is fitted around a laminated target on the shaft and are wired to form a bridge arrangement in each of the 2 axes of the radial bearing. Each axis has as a minimum an opposed pair of sensing elements, where each element is a variable inductor incorporating the rotor/stator air gap, such that variations in gap result in variations in inductance. The sensor is then driven with a balanced AC drive signal which may be either sinusoidal or a square wave. Waukesha prefer sinusoidal drive due to the linear behavior of such systems. The drive frequency is selected to be as high as possible whilst still working within the "inductive" frequency range of the sensor elements. If the drive frequency is set too high then the elements are affected by eddy currents and resonance with cable capacitance.

The radial sensor in figure 1 has single wound coils giving a single ended signal relative to the center point of the drive signals, Alternative dual wound arrangements are possible which provide a differential output from the sensor ring, giving improved noise immunity. In either case, the resulting output from the sensor ring is a waveform whose amplitude is a function of the displacement of the rotor away from the center of the sensor ring and the phase of the waveform relative to the drive waveform is nominally either 0° or 180° depending on the direction of the displacement. When the rotor is centered in the sensor ring the output should be zero.

The schematic of a typical axial sensor arrangement is shown in figure 2.

Because the output of the bridge is phase sensitive, phase sensitive de-modulation of the sensor signal is required. This may be performed either using analogue electronics or digitally. Waukesha use convolution techniques as shown in Figure 3 to perform the phase sensitive demodulation. Jayawant and Dabbs (Jayawant R. a., 2013) describe a digital phase sensitive demodulation circuit.

Whichever method is chosen, the signal must be within the working range of the de-modulation circuit

Within this whole arrangement, there are several sources of noise and other non-ideal behavior, which can be seen in Figure 4:

1. Common mode noise. For the single wound sensor arrangement, each output signal is referenced relative to the mid-point of the balanced drive waveform (which is derived within the AMB controller). Consequently, any common mode noise which couples into the sensor signal may result in a measurement error. However, the de-modulation circuit will have a limited bandwidth (typically $1/10^{th}$ of the carrier frequency) and so out of band noise will not impact on the resulting measured signal. The dual wound sensors are immune to common mode noise and so are better suited to systems with long cable runs.

2. Bandwidth. The bandwidth of the sensor is limited by the bandwidth of the de-modulation circuit, which in turn is limited by the carrier frequency, since we will normally want to limit the amount of carrier frequency "breaking through" into the output waveform. As previously noted, eddy current and resonance effects limit the carrier frequency.

3. Electronic noise. For analogue de-modulation and the analogue front end of digital demodulation circuits, the circuits will have electronic noise added into the waveform at each stage. The larger the waveform we are working with, the lower will be the impact of the noise. However, we need to ensure the signal remains within the working voltage of all circuits in order to avoid clipping and the resulting non-linear behavior.

4. Quantization noise. For digital demodulation, the waveform will be sampled through an A to D converter (ADC). This will result in quantization noise. We want to have as many "counts" as possible across the working range of the sensor. This may be achieved by either having an ADC with a higher resolution or by optimizing the gains in the sensor system so that the resulting signal corresponds with the range of the ADC when the rotor is traversed across working range of the sensor. Use of a high resolution ADC may not be available for some Digital Signal Processors (DSPs) and will incur extra cost.

5. Other sources of noise can be attributed to the electro-mechanical assembly of the sensing elements and rotor system. Differences in positioning and inductance of the sensor elements can result with signal distortion and increased level of sensors noise. Additional sources of noise, identified during rotation, are attributed to uneven surface of the rotor lamination target in the rotor. These geometric defects manifest as rotor runout, produced during the machining. Operation of the rotor, or localized rotor lamination defects, light dents or scratches, produced during assembly or operation. These type of noise effects can be mitigated by the mechanical configuration of the sensor elements, increasing the number of the sensing elements, or digitally with filtering algorithms embedded in the control structure.

A typical AMB system will have an associated touchdown bearing system (TDB) which will limit the rotor motion in the event of failure of the AMB. The motion of the rotor is limited by the clearance within the TDB together with the compliance of the TDB. It is noted that the clearance of the AMB magnets and sensors is typically much larger than the TDB clearance.

An AMB system will normally be set up so that the "zero" positions are when the rotor is centered in the TDBs.

It is imperative that the sensor is able to provide a valid signal across the whole range of motion (clearance plus compliance) and a small margin is typically added to allow for thermal effects, wear in the TDB and rotor and housing deflection. For Waukesha this results in a design guideline that the sensor working range should be 1.5 to 2 times the TDB allowable movement (clearance plus compliance).

The sensor rings and the TDBs are separate parts within the AMB / machine assembly and will have non-concentricity to each other. The novel sensor circuit described in this paper mitigates the negative impact on required sensor working range of such non-concentricity.

2 The Results of Misalignment with Touch-Down Bearings

The mechanical hardware of a magnetic bearing system typically consist of assembled components, including actuator, sensor and auxiliary bearings, assembled in stacked configuration, as represented in Figure 5. Due to the manufacturing tolerances associated to each component, some residual misalignment is always present between these components. While axial misalignment can be partially corrected with shims or spacers between the stacked components, the radial misalignment is more problematic. Tight machining tolerances, manufacturing and assembly procedures can be applied to correct radial misalignment but this results with additional cost and assembly time.

For an ideal AMB supported rotor system, the two radial sensor stators will be concentric with the two radial TDB. In this case, when the rotor is centered in the TDB, it will be centered in the sensor rings. When centered, the bridge circuit formed by the inductive sensors for the given axis will be balanced and the output of the bridge will be zero as shown in Figure 6.

Also shown in Figure 6, we see that if the rotor is displaced in the +ve direction to the TDB clearance we will get an amplitude Y. If the rotor is displaced to the TDB clearance in the –ve direction, we will get the same amplitude, but out of phase by 180°. In this case we can set up the gain at the front end of the de-modulation circuit so that (nominally) the amplitude Y corresponds to the input range of the ADC or the analogue de-modulation circuit.

Remembering that the clearance in the AMB magnets and the AMB sensors may be several times that of the TDB, we now consider the case where the radial sensors stators are not concentric with the TDB stators. In Figure 7, we show the (extreme) case where the sensors are non-concentric with the TDB by twice the TDB clearance.

When centered at the TDB, the bridge circuit formed by the inductive sensors for the given axis will no longer be balanced and the output of the bridge will have amplitude 2Y as shown in Figure 7.

Also shown in Figure 7, we see that if the rotor is displaced in the +ve direction to the TDB clearance we will get an amplitude 3Y. If the rotor is displaced to the TDB clearance in the –ve direction, we will get amplitude Y with the same phase.

In order for the sensor range to be operational over the range of TDB motion, the gain at the front end of the de-modulation circuit needs to be set so that a signal of amplitude 3Y can be correctly processed. This means the sensitivity compared to the well centered case is reduced (in this case) by a factor of 3, with a corresponding increase in quantization and other electronic noise. It should also be noted that 2/3 of the sensor range is not used.

3 Overview of the Novel Sensor Input Circuit

The circuit shown in figure 8 allows the effect of the non-concentricity between the sensor stator and the TDB stator to be compensated electronically, giving a well centered signal with respect to motion within the TDB clearance. Because the signal is well centered, it is then possible to optimize the gain to fully use the input range of the phase sensitive sensor demodulation circuit.

The way the patented (UK Patent No. GB2582286, 2021) circuit works is to apply an “offset” level of a copy of the drive waveform to each incoming sensor output signal. The offset signal will either be in phase with the drive waveform or 180° out of phase with the drive waveform. The amplitude of each offset is adjusted so that the relevant signal is well centered.

The summing amplifiers which combine each sensor signal with the relevant offset, need to be of sufficient dynamic performance (bandwidth and slew rate) and input range to be able to handle the two signals without clipping, distortion or other signal degradation. Because the bandwidth of this input circuit is likely to be many times the carrier frequency, the impact on the overall sensor system bandwidth of this circuit will be insignificant. If the gains, “gain1” and “gain2” of Figure 8 are made to be variable, then the signal can be optimized for the input range of the signal processing

circuit (in Figure 8 the ADC). If the gains are combined with the summing amplifiers then any concerns regarding "clipping" of the input signal can be eliminated.

The resulting (idealized) waveforms are shown in figure 11. These show the sensor output of Figure 7 after suitable compensation, together with the waveforms at the ADC input after suitable gain adjustment. In this case, we have assumed an ADC input range of +/-8Y as shown in the figure. The offset and gain have been adjusted so the sensor has been setup with 7/8 of the ADC range corresponding to the maximum TDB motion (as an example).

The circuit shown in figure 8 shows "single ended" sensors. For a dual wound differential sensor, the differential signal would be combined together with the offset to give the compensated signal.

In all of the examples so far, the sense signals have been in phase with the drive waveform. In a real world application, the sense waveforms will be phase shifted from the drive due to resonance effects from the cable capacitance in parallel with the sensor inductance.

The circuit presented here is able to compensate the in-phase component of the waveforms. In the example in Figure 12, the sense signal is shifted by 15°. In Figure 12, we can see the resulting waveforms, together with the in-phase component of the resulting signals. The gain applied to the signal again results in a maximum amplitude of 7Y, but the useful component now has a maximum amplitude of approximately 6Y i.e. 1/7 of the ADC range is not used. This is still significantly better than the case where no correction is applied where 2/3 of the ADC range is effectively unused.

In the extreme case where the phase shift is 90°, then the circuit would not be able to compensate for TDB offset, however, phase shifts of this magnitude have not been observed within the author's Company.

Algorithms and circuits with variable phase shift on the offset have been investigated, but the algorithms required for setup become overly complex and result in excessive configuration time. Practical experience shows that this capability is also not needed.

4 Deployment of the Sensor Circuit in a New AMB Controller Designed for Low-Cost Machinery

The first deployment of the novel sensor circuit was into a compact AMB controller designed for low cost machinery. Designated Alisio™, the controller includes the fully digital demodulation circuit presented by Jayawant and Dabbs (Jayawant R. a., 2013), together with the gain and offset adjustments presented here. Figure 13 shows the controller (with its enclosure removed) and Figure 15 shows the sensor card which includes the novel sensor circuit.

The sensor card also includes signal conditioning for PT100 temperature sensors and dual speed sensors.

The controller is available in two build configurations, a low power 1KVA version and a 2KVA version. The 1 KVA version has 10 magnet drives, each with a 300V DC link and maximum continuous output current of 3A. The 2KVA version has the same DC link but with 5A maximum continuous output current. In both cases the peak current is still being refined, but is expected to be 4A and 6A respectively.

The remaining major specifications related to the position sensor sub-system are shown in table 1.

The digital demodulation circuit presented by Jayawant and Dabbs (Jayawant R. a., 2013) is shown in Figure 14. When combined with the Software controlled Offset and Gain, this allows the full sensor setup to be performed remotely under the control of the Waukesha magBOOST™ automated commissioning tools.

The first application of the Alisio™ controller was into a centrifugal compressor for a chiller application.

In this case, the mechanical components for the actuator, sensor and auxiliary bearing were stacked together and the relative centering resulting from the manufacturing tolerances of the individual components and the positioning of the axial shims. For these type of AMB systems,

normally intended for high volume applications, although the axial centering of the auxiliary bearing and position sensor can be adjusted with a set of mechanical shims, the correction of the centering with an electronic system provides a faster and more economical way to adjust the axial concentricity without an additional set of shims.

Table 1 - Alisio™ Specification

Function	Specification
Controller Sample rate	15 KHz (upgrade to 20KHz planned)
Sensor sample rate	210KHz
Sensor carrier frequency	26.25KHz
Input Adjustment functions	Software controlled offset and gain using digital potentiometers.
Phase sensitive demodulation	Fully digital with fully adjustable phase
Dimensions (3A version)	292 x 239 x 86.5 mm
Cooling (3A version)	Cold plate mounted
Maximum Cold plate temperature (3A)	60 °C

5 Techniques for Automatic Configuration of the Sensor Input Circuit

The sensor input circuitry is set up by moving the rotor within the TDB clearance (and compliance), providing measurement points for varying position. So that valid measurements are obtained, it is important to ensure that the input signal does not saturate whilst still maintaining as large a signal as possible. In order to do this, the phase sensitive de-modulation circuit is used to evaluate the amplitude of the signal at each measuring point. The phase is swept through 360° and the peak response at each measurement point will give the magnitude and phase of the relevant measurement. If the response at any of the measurement points is larger than the permitted level then the gain of the input circuit is reduced until a valid measurement can be obtained at all measurement locations.

There are various techniques for moving the rotor within the TDB clearance:

1. Single axis open loop clearance check

With this technique, open loop current is driven in the magnets of a given bearing axis to pull the rotor around within the TDB clearance. This technique can be used for the initial configuration of the sensor system. This is shown schematically in figure 9.

2. Partially Levitated Clearance check

This technique uses levitation on all axes except one, with the remaining axis pulled within the TDB clearance using open loop current. This is shown in Figure 10. This technique will normally be iterated twice across the axes to obtain the optimal settings.

Now that we are able to move the rotor within the TDB clearance, the sensor configuration techniques follow.

For each axis, we start with a low gain setting and zero offset. Pulling the rotor will yield two measurement points P1 and P2. These are shown in the argand diagram of Figure 16. We then apply the offset to bring the vector of the mid-point P3 so that it is orthogonal to the vector between the 2 measurement points (also shown in figure 16). Resulting in points P1', P2' and P3'. We note that the magnitude of P1' and P2' are now equal. Once we have the correct offset applied, we can then adjust the gain to bring the amplitude of the signal at the two extreme positions (P1' and P2')

to the desired value. This method is only applicable to small angles β. At angles above 30°, the length of the vectors P1' and P2' will start to diverge and at angles above 60° we may see vectors with magnitude greater than the original vectors.

The techniques described above, including:

a. Using the phase sensitive de-modulation to evaluate the amplitude and phase at each measurement point;
b. Adjustment of gain to ensure all measurements are valid;
c. Single axis open loop clearance check;
d. Partially levitated clearance check;
e. Computation of offset;
f. Computation of gain;

are all fully automated within the Waukesha magBOOST™ automated commissioning tools (described by Jayawant and Daves) (Jayawant R. a., 2013) allowing for rapid execution of this relatively complex procedure.

6 Results from prototype testing

Prototype testing with 3 machines was conducted. These were commissioned remotely (including the initial sensor setup) which was conducted using the Waukesha magBOOST™ automated commissioning tools. In particular, use was made of the single axis open loop clearance check function. Each axis had 2 measurement points, one with current in the "top" magnet flowing and one with current in the "bottom" magnet.

Table 2 - Analysis of Axial Signals Before and After Application of Offset.

Original Measurement				offset (Count)
Bot Magnet pull		Top Magnet pull		
Mag (count)	phase (°)	Mag (count)	phase (°)	
257562	180	132373	191	188474
246595	180	102635	180	174615
272130	191	100968	180	200920

Final Configuration				Increased gain which can be applied
Bot Magnet pull		Top Magnet pull		
Mag (count)	phase (°)	Mag (count)	phase (°)	
69088	180	64079	-24	3.73
71980	180	71980	0	3.43
84687	-141	99952	0	2.72

The currents were set so as to be able to lift the rotor. However, when pulling with the top magnet in a radial axis, it may not be possible to fully displace the rotor in the direction of the relevant axis due to gravity and the resulting force vector at the contact point within the TDB. This effect is not relevant to axial bearings. For the initial set-up this effect is considered not significant and would be eliminated in the subsequent partially levitated clearance check. Unfortunately, at the time of writing this paper, the results from the partially levitated clearance checks were not available.

It is noted that in these machines the controller is integrated with each machine and consequently very low cable capacitance results. Figure 17 shows the useful vector for the various axes and

Figure 18 shows the ratio of the useful vector and the actual offset vector for each of the axes, i.e. the ratio of the amplitudes and the relative phase angle between the two vectors.

We can see that all of the useful vectors lie close to the x-axis. We can also see that the offset on the axial axis in all three cases has greater magnitude than the useful signal, but is close to -180° and so is eminently correctable using the new input circuit.

We will look at what happens when we apply the optimal correction using the technique of Figure 16 to the measured axial signals.

Table 2 shows the original measured signals together with the optimal correction and the resulting signals. The table also shows the increased level of gain that can be applied prior to the ADC (compared to the case where the offset is not present).

7 Conclusions and Future Work

The use of the patented offset circuit allows for relaxed tolerancing in the mechanical build, leading to faster build times and reduced costs. The normal down side to this relaxed tolerancing (sensor offset) is compensated by the new circuit, allowing larger gain to be applied to inductive sensor signals prior to processing by demodulation circuits (either analogue or digital). This increased gain allows similar performance (with regard to quantization and other electronic noise present within the sensor demodulation circuits) compared to a tightly tolerance system.

Tests on prototype systems allowed increased gain of between 2.7 and 3.5 to be applied to the axial sensor signals prior to A to D conversion compared to the case where the offset circuit was not present.

The use of software controlled gain and offset adjustments when combined with the fully digital phase sensitive de-modulation circuit supports the fully remote commissioning model, particularly when supported by sophisticated automated commissioning tools such as the Waukesha magBOOST™ software.

Further work (ongoing and planned) includes:

- Systematic measurement of noise levels with and without the offset deployed.
- Incorporation of the offset circuit into the Zephyr™ AMB controller. This is in progress and expected to be available in Q3 2021.
- Evolution of algorithms for computation of offset when the useful vector has a large phase angle.
- Testing with longer cables where phase shifts may be more significant. This is waiting on completion of the work on the Zephyr™ controller.

References

Jayawant, R. and Dabbs, S., (2013). A Novel Digital Circuit for Position Sensor De-modulation Using Advanced FPGA, Including Field Experience with a 1.45MW Motor Driven Compressor. *Proceedings of the 1st Brazilian Workshop on Magnetic Bearings, Rio de Janeiro, 2013.* Rio de Janeiro: Available at http://www.magneticbearings.org/publications/.

Jayawant, R. and Davies, N., (2013). Integration of signal processing capability in an AMB controller to support remote and automated commissioning. *Proceedings of the 1st Brazilian Workshop on Magnetic Bearings.* Rio de Janeiro: Available at http://www.magneticbearings.org/publications/.

Leung, C. and Davies, N.,. (2021). *UK Patent No. GB2582286.*

Traxler, A. and Maslen, E.,. (2009). Hardware Components. In Schweitzer, G. and Maslen, E., *Magnetic Bearings* (pp. 101-102). Zurich: Springer.

Figures

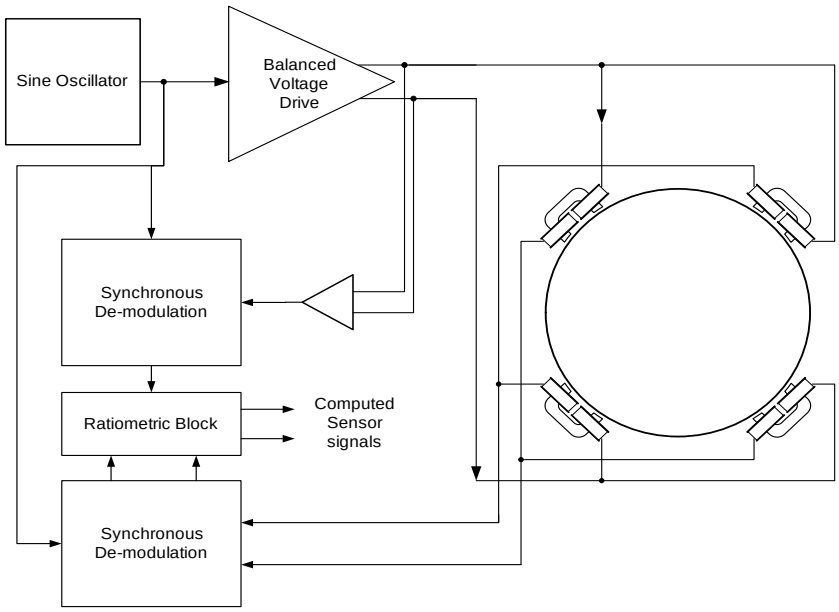

Figure 1 - Radial Inductive Sensor Schematic

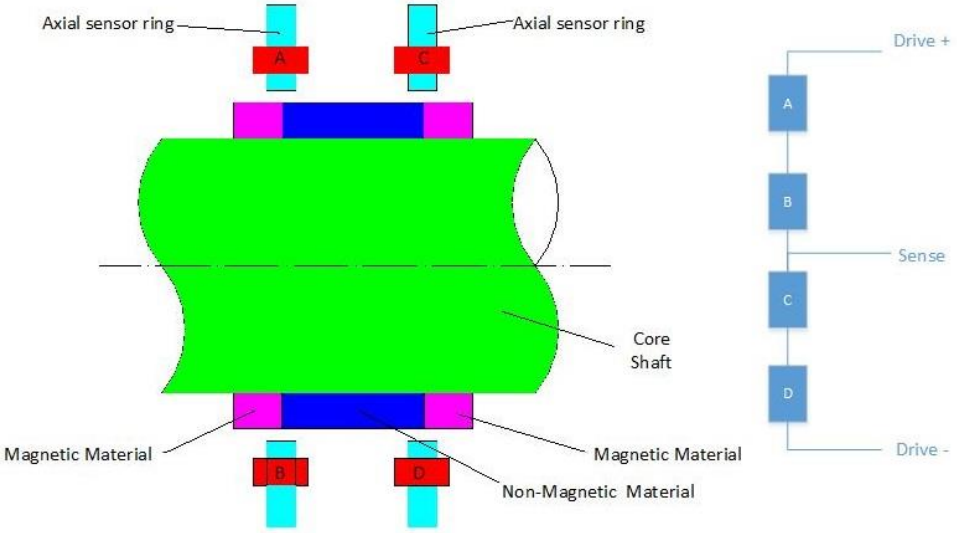

Figure 2 - Axial Inductive Sensor Schematic

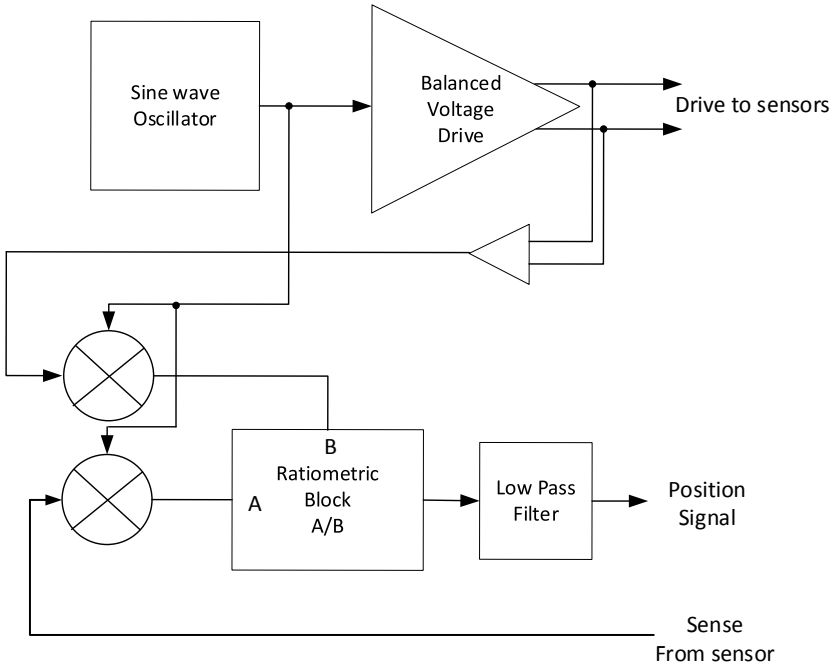

Figure 3 - Analogue Phase Sensitive Demodulation.

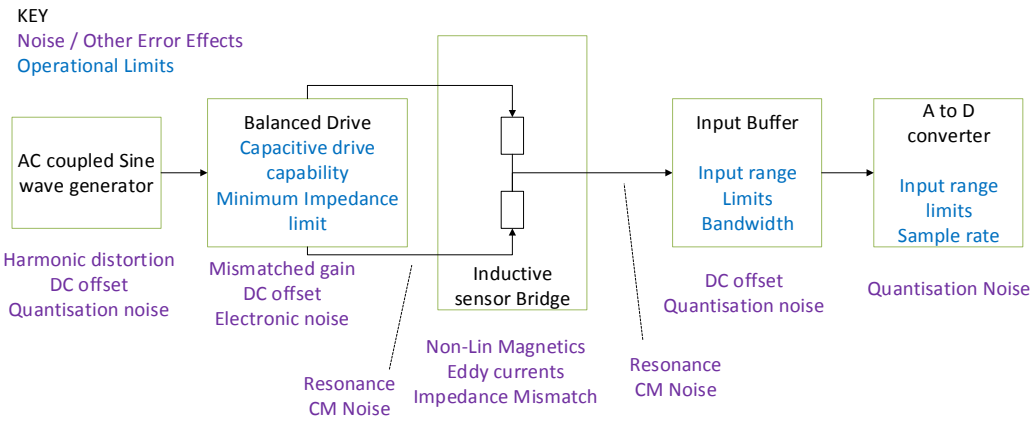

Figure 4 - Constraints within the Signal Processing Circuit and Sources of Noise.

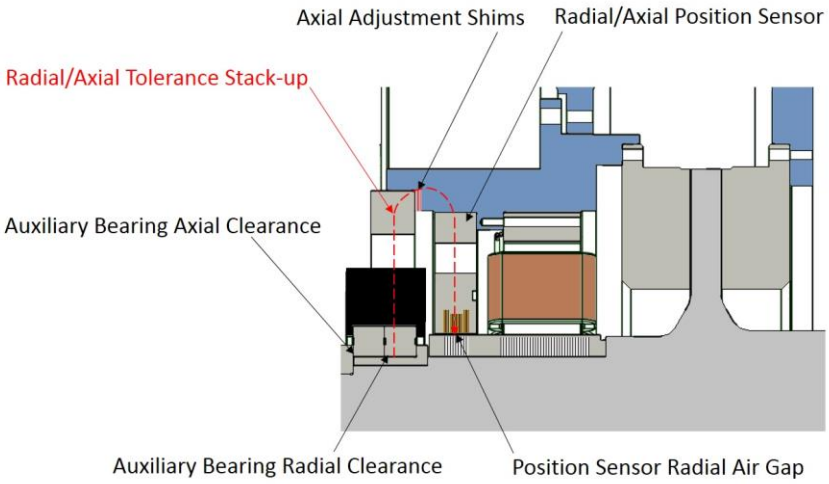

Figure 5 - Non-Concentricity Due to Non-Concentricity in the Housing or AMB Components.

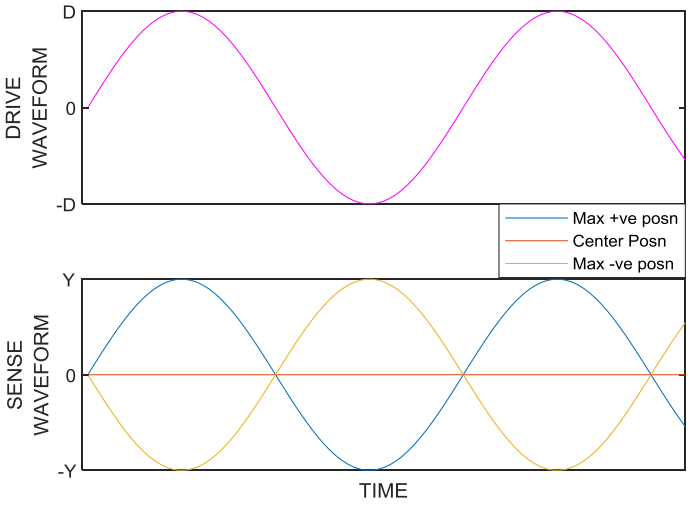

Figure 6 - Ideal Signals from a Well-Centered Sensor Ring.

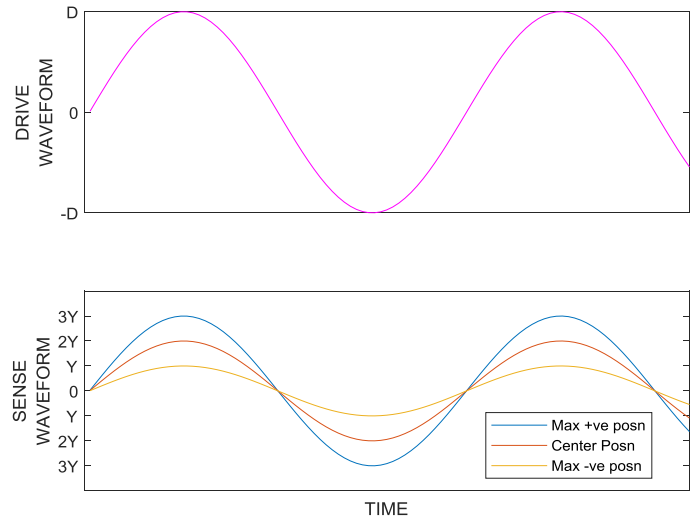

Figure 7 - Signals from a Non-Concentric Sensor Ring.

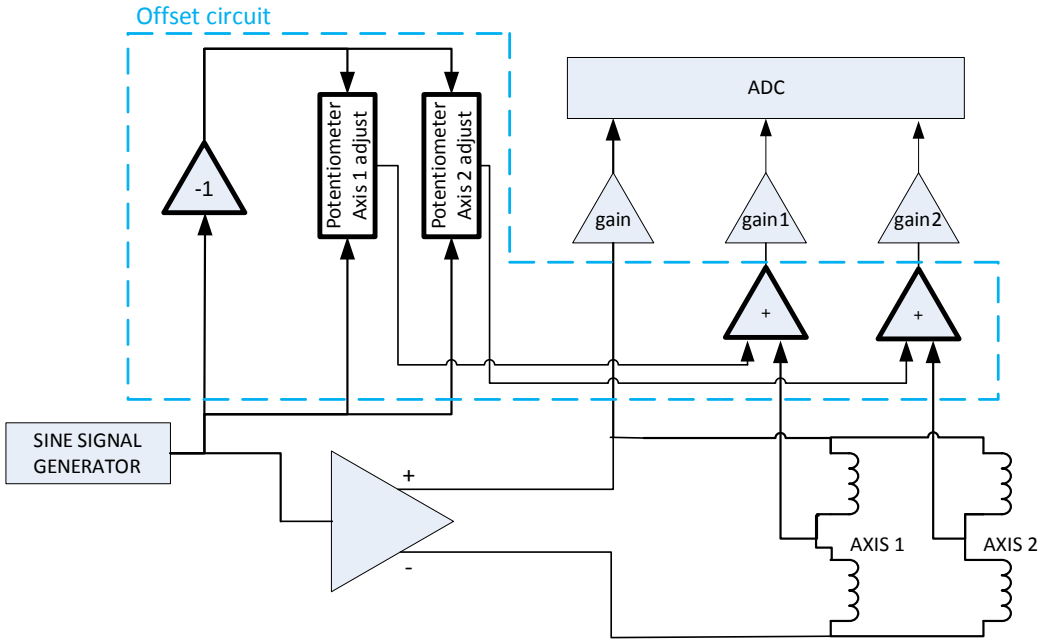

Figure 8 - . Schematic Diagram of the Sensor Input Circuit.

Figure 9 - Single Axis Open Loop Clearance Check.

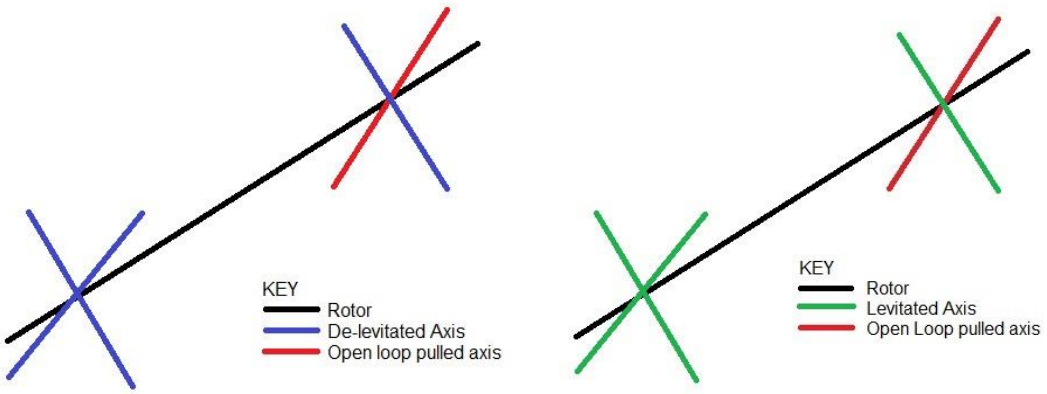

Figure 10-Partially Levitated Clearance Check.

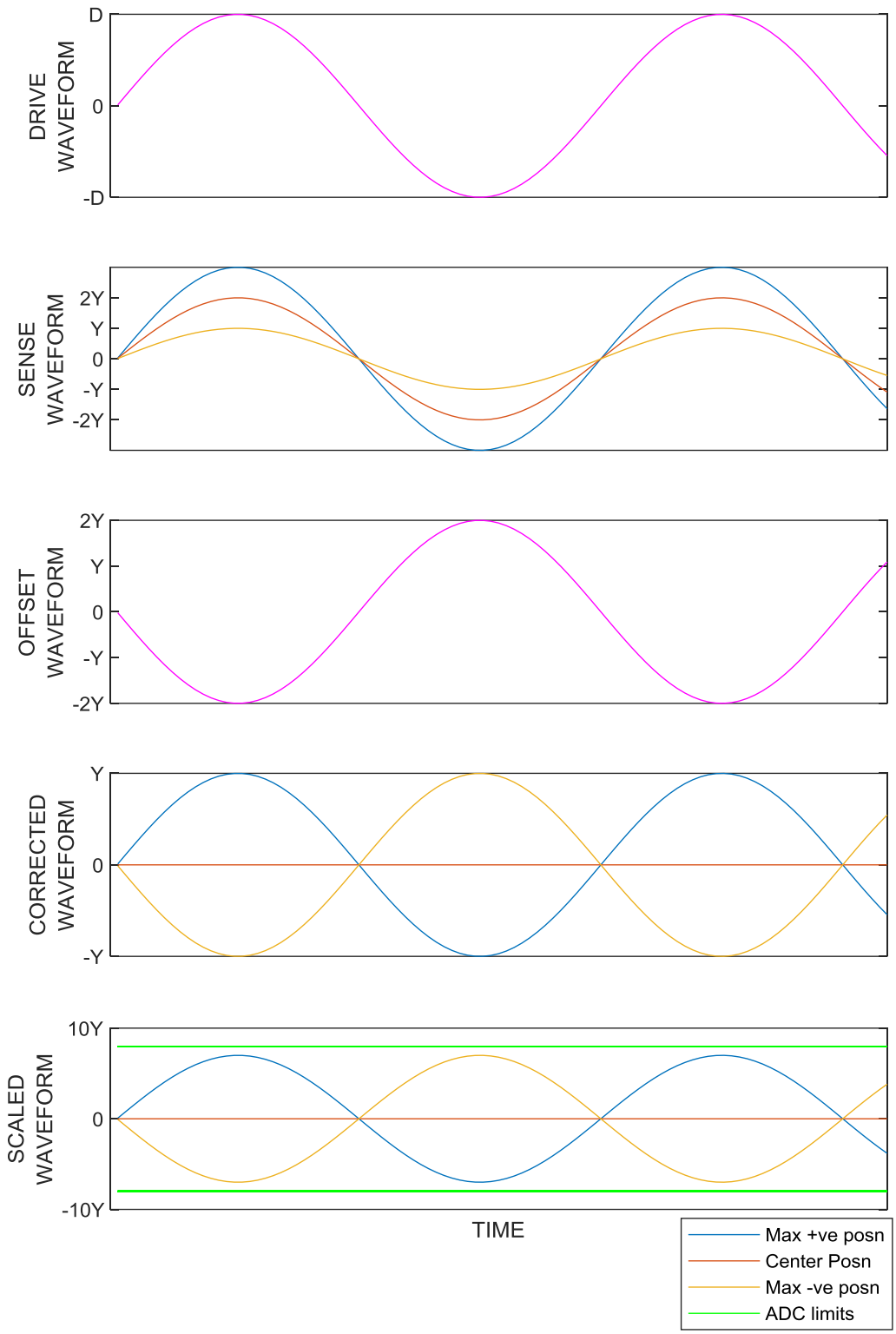

Figure 11 - Sensor Waveforms as Modified by the Sensor Input Circuit.

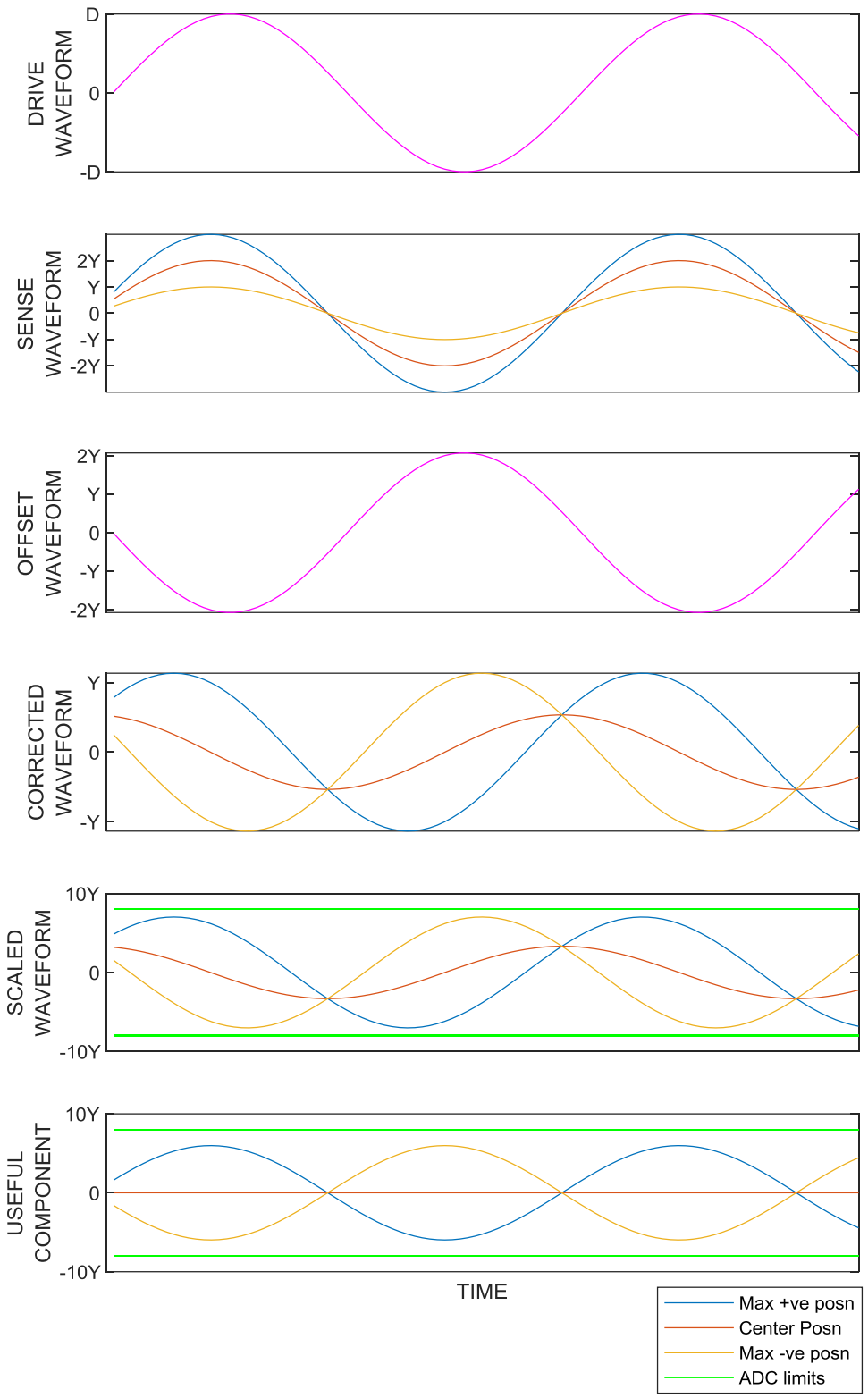

Figure 12 - Sensor Waveforms when the Sense Signal Is Out of Phase with the Drive Signals.

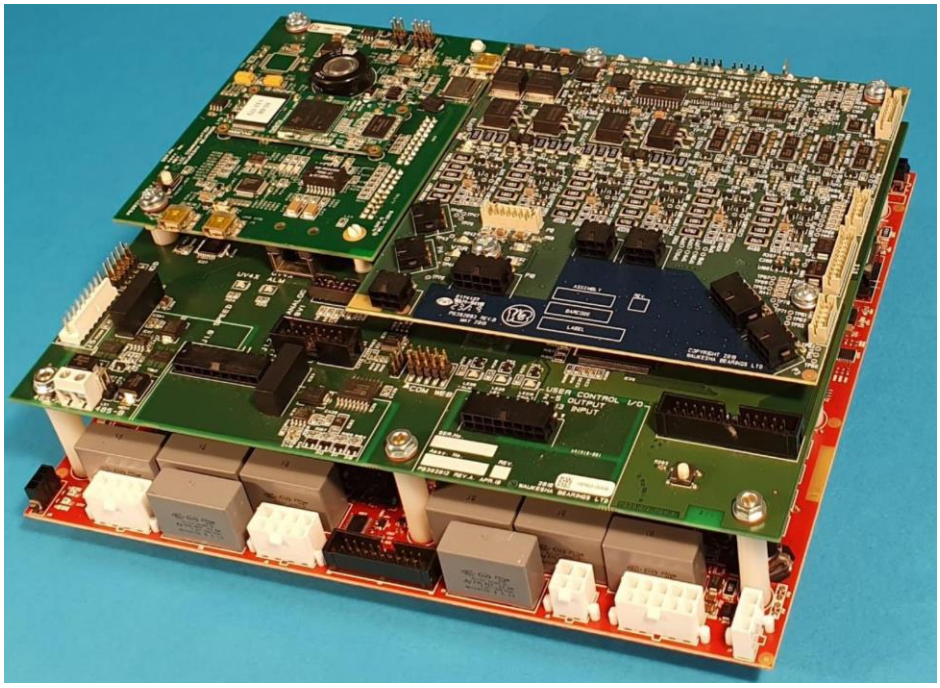

Figure 13 - Alisio™ Controller (enclosure removed).

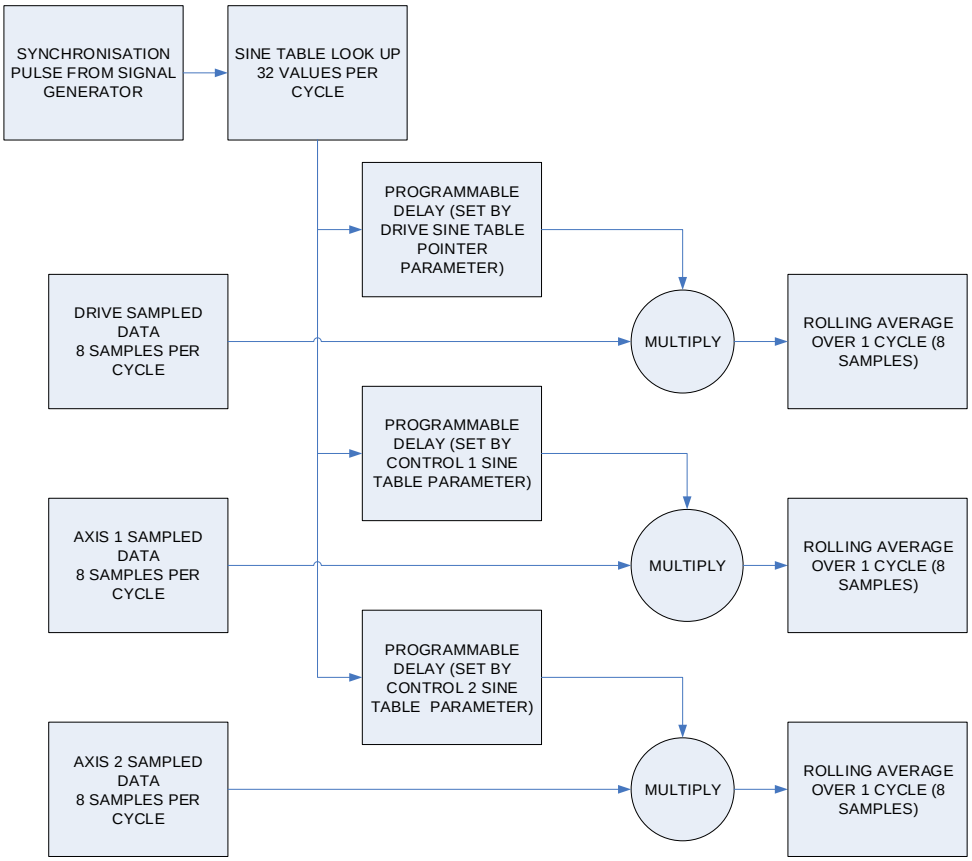

Figure 14 - Digital Phase Sensitive Demodulation.

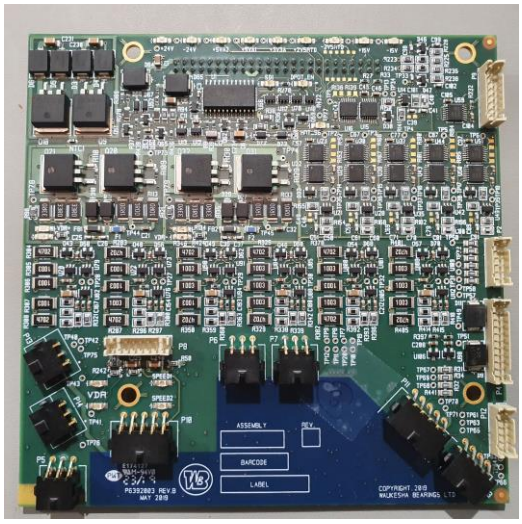

Figure 15 - Alisio™ Sensor Card.

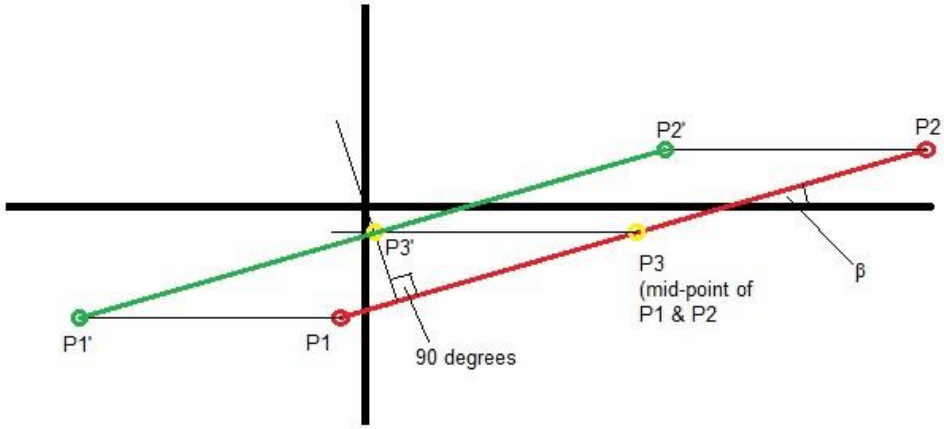

Figure 16 - Argand Diagram Showing Calculation of Offset.

Figure 17 - Argand Diagram Showing Useful Vector for the Various Axes

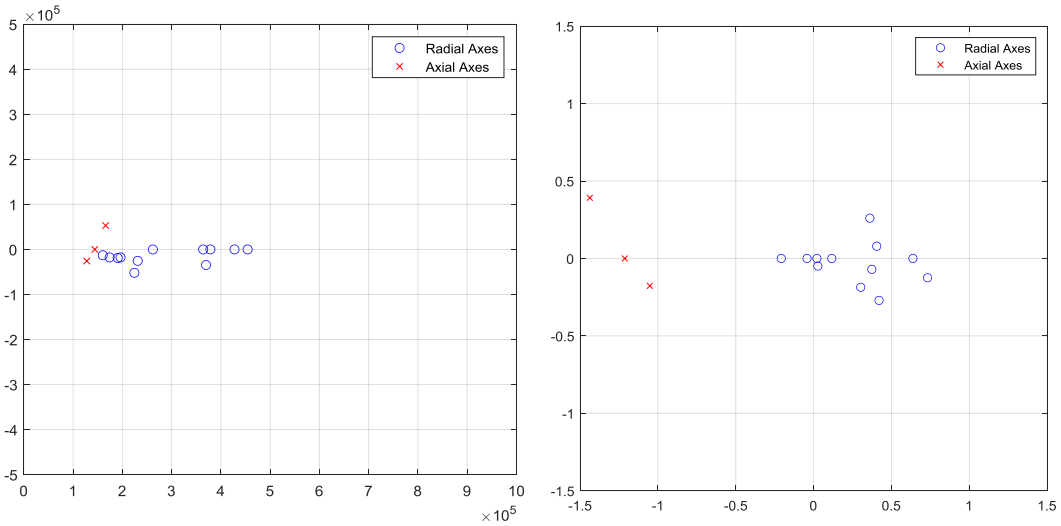

Figure 18 - Argand Diagram Showing Relative Magnitude and Phase of Actual Offset Vector and Useful Vector (Offset/Useful)